Cell

Article

A Noncanonical Frizzled2 Pathway Regulates Epithelial-Mesenchymal Transition and Metastasis

Taranjit S. Gujral,[1] Marina Chan,[1] Leonid Peshkin,[1] Peter K. Sorger,[1] Marc W. Kirschner,[1,*] and Gavin MacBeath[1,*]
[1]Department of Systems Biology, Harvard Medical School, 200 Longwood Avenue, Warren Alpert 524, Boston, MA 02115, USA
*Correspondence: marc@hms.harvard.edu (M.W.K.), gavin_macbeath@harvard.edu (G.M.)
http://dx.doi.org/10.1016/j.cell.2014.10.032

SUMMARY

Wnt signaling plays a critical role in embryonic development, and genetic aberrations in this network have been broadly implicated in colorectal cancer. We find that the Wnt receptor Frizzled2 (Fzd2) and its ligands Wnt5a/b are elevated in metastatic liver, lung, colon, and breast cancer cell lines and in high-grade tumors and that their expression correlates with markers of epithelial-mesenchymal transition (EMT). Pharmacologic and genetic perturbations reveal that Fzd2 drives EMT and cell migration through a previously unrecognized, noncanonical pathway that includes Fyn and Stat3. A gene signature regulated by this pathway predicts metastasis and overall survival in patients. We have developed an antibody to Fzd2 that reduces cell migration and invasion and inhibits tumor growth and metastasis in xenografts. We propose that targeting this pathway could provide benefit for patients with tumors expressing high levels of Fzd2 and Wnt5a/b.

INTRODUCTION

The epithelial-mesenchymal transition (EMT) is a reversible process in which epithelial cells adopt mesenchymal properties by altering their morphology, cellular architecture, adhesion, and migratory capacity (Lee et al., 2006). EMT was originally defined in the context of metazoan developmental stages, including heart morphogenesis and mesoderm and neural crest formation (Savagner, 2010). A similar process (also called EMT) is activated during the development of organ fibrosis and wound healing (Thiery et al., 2009). During tumor progression, EMT allows benign tumor cells to infiltrate surrounding tissue and metastasize to distant sites. More recently, several studies have postulated a link between EMT and stem cell characteristics (Gupta et al., 2009), as well as drug resistance, reinforcing the idea that EMT is closely linked to morphogenesis and tumor progression (Thiery et al., 2009).

Induction of EMT involves downstream transcription factors, such as Snail and Twist, as well as cytokines, such as MMP2 and MMP9. Several growth factors, including TGFβ, Wnt, EGF, FGF, and HGF, have been shown to trigger EMT in both embryonic development and normal and transformed cell lines (Thiery et al., 2009). However, mechanistic understanding of how specific growth factors induce EMT is still lacking. Uncovering the signaling pathways by which growth factors regulate EMT could have broad biological significance and could potentially guide the development of new therapies directed at cancer metastasis.

In this paper, we study the role of Wnt signaling in the regulation of EMT and cancer metastasis. Wnt family proteins are growth factors that play critical roles in proliferation, migration, and invasion. They bind to and activate one or more of ten known seven-transmembrane Fzd family receptors (Willert et al., 2003). Defective Wnt signaling plays a critical role in the early stages of colon cancer (Klaus and Birchmeier, 2008). For example, >90% of all sporadic colon cancers feature aberrant Wnt signaling, usually as a result of mutations in genes encoding adenomatous polyposis coli (APC; 80%), β-catenin (CTNNB1; 10%), or Axin (Giles et al., 2003). Many previous studies have uncovered activation of canonical Wnt/βcatenin signaling during EMT (Deka et al., 2010; Gupta et al., 2010; Wu et al., 2012). These studies show that, during the EMT process, there is an increase in nuclear β-catenin (likely due to loss of membranous E-cadherin) and transcriptional activity of T cell factor (TCF). However, it is not clear whether EMT is directly caused by ligand-driven canonical signaling. Upregulation of noncanonical Wnt ligand (Wnt5a) and activation of noncanonical Wnt components, including PKC and JNK, have also been observed during EMT (Dissanayake et al., 2007; Jordan et al., 2013; Scheel et al., 2011). However, a mechanistic understanding of how Wnt5a induces EMT and whether it is canonical or noncanonical, or whether it is by any previously identified pathway, is left unanswered by previous investigations.

We systematically assessed Wnt and Fzd transcripts in a variety of cancer cell lines and correlated their levels with epithelial and mesenchymal markers. We found that the Wnt5a and Wnt5b ligands, along with their cognate receptor Fzd2, are generally overexpressed in cell lines derived from late-stage mesenchymal-type hepatocellular carcinomas (HCC) and cancers of the breast, lung, and colon. Fzd2 was also overexpressed in late-stage clinical cases of HCC and lung cancer, and overexpression was correlated with poor patient survival. Reducing receptor expression by RNAi or blocking receptor activity with anti-Fzd2 antibodies reduced Wnt5-mediated cell migration

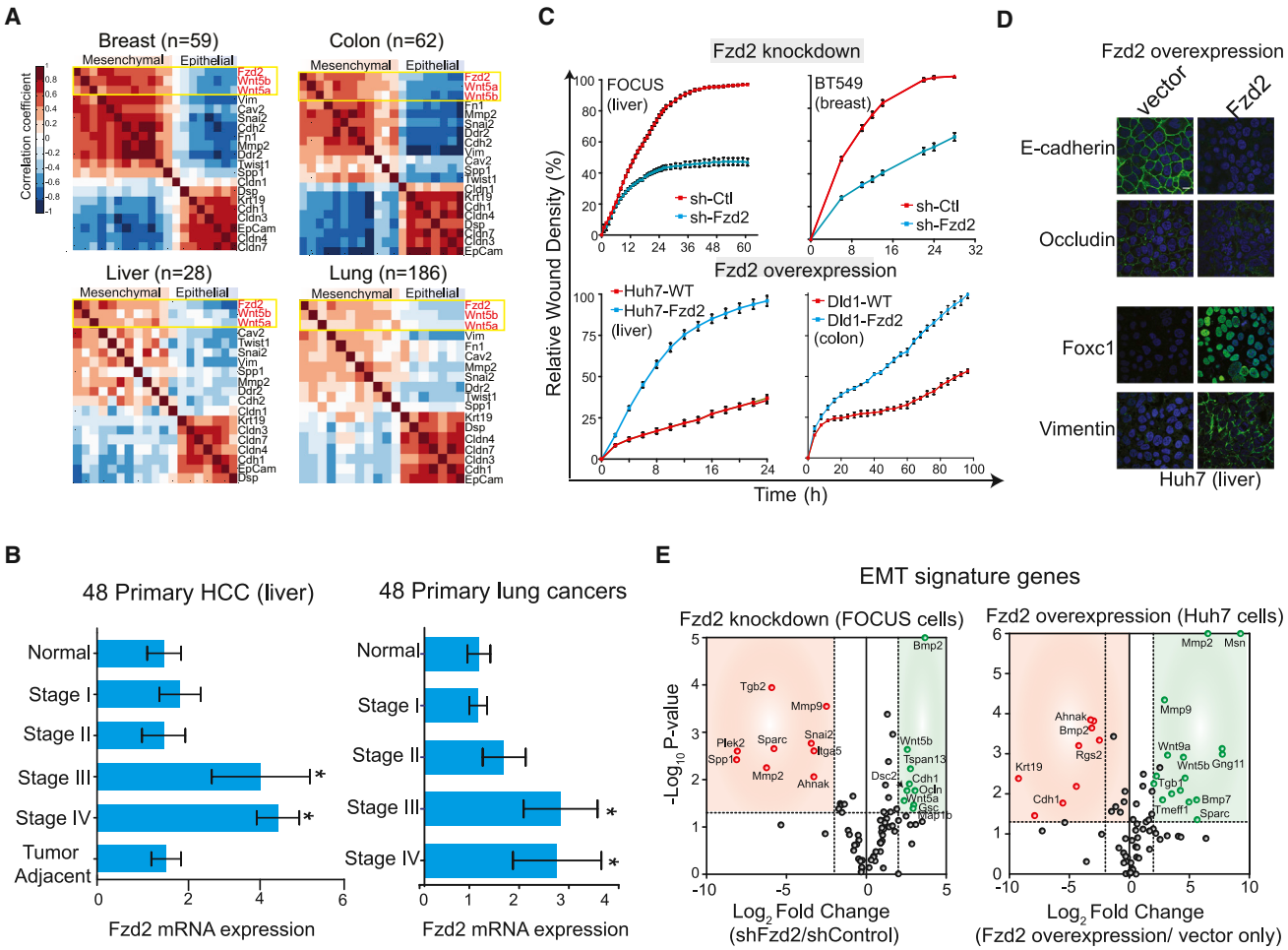

Figure 1. Fzd2 and Its Cognate Ligands Wnt5a/b Are Overexpressed in Late-Stage Cancers, and Their Expression Correlates with Mesenchymal Markers

(A) Heatmaps showing correlation of Fzd2 and its ligands Wnt5a/b with mesenchymal markers in 59 breast, 62 colon, 28 liver, and 186 lung cancer cell lines.

(B) Bar graph showing that Fzd2 mRNA expression is significantly increased in late stages (stages III and IV) of primary liver and lung cancers compared with normal tissue ($p < 0.05$).

(C) Fzd2 regulates cell migration. Top, relative wound density (RWD) of Fzd2-shRNA- or control-shRNA- (sh-Ctl) expressing FOCUS and BT549 mesenchymal cells. Bottom, RWD of Fzd2-expressing or control vector-expressing Huh7 and Dld1 epithelial cells. RWD is a measure of the spatial cell density in the wound area relative to the spatial cell density outside of the wound area at every time point.

(D) Fzd2 signaling regulates EMT program. Representative images showing that expression of Fzd2 in Huh7 cells decreased levels of the epithelial markers E-cadherin and Occludin and increased levels of the mesenchymal markers Foxc1 and Vimentin. Blue, nucleus stain.

(E) Volume plot of 75 EMT genes measured by qPCR in FOCUS cells expressing Ctl-shRNA or Fzd2-shRNA (left) or Huh7 cells expressing vector only or Fzd2 expression vector (right). A set of genes that were significantly downregulated ($p < 0.05$) upon knockdown of Fzd2 are shown in red, whereas significantly upregulated ($p < 0.05$) genes are shown in green.

Error bars indicate SEM. See also Figures S1 and S2.

in vitro and inhibited tumor growth and metastasis in a mouse xenograft model. Further analysis of the pathway leading from Fzd2 to migration revealed a role for several previously unrecognized molecules, including Fyn, a Src family kinase, and Stat3, a transcription factor. These data establish a noncanonical Wnt pathway involving Fzd2 receptor, Fyn tyrosine kinase, and the Stat3 transcriptional regulator as a driver of EMT in diverse solid tumors; cell culture and murine experiments highlight Fzd2 as a potential therapeutic target for late-stage and metastatic cancer.

RESULTS

Fzd2 Is Overexpressed in Poorly Differentiated, Mesenchymal-type Cancers

To probe the roles of Wnt and Fzd proteins in EMT, we assessed gene expression levels for 16 Wnt ligands and 10 Fzd receptors in 27 HCC cell lines (Figures 1A and S1 available online) (Barretina et al., 2012). Based on morphology and expression of biomarkers such as E-cadherin and vimentin, these lines span a range of phenotypes from well to moderately differentiated and

epithelial like to poorly differentiated and mesenchymal like (Fuchs et al., 2008). A statistical information-gain approach revealed that the expression level of *Fzd2* is the best single-gene discriminator of poorly versus well-differentiated HCC cell lines in our collection (Figure S1). In addition, ligands for Fzd2 receptor (*Wnt5a* and *Wnt5b*) were more highly expressed in poorly differentiated cell lines than in well-differentiated lines (Figure S1). Expression of *Fzd2* and its cognate ligands (*Wnt5a* and *Wnt5b*) correlated positively with each other and with markers of mesenchymal cells, such as vimentin (*VIM*), N-cadherin (*CDH2*), and fibronectin (*FN1*), in panels of breast (n = 59), colon (n = 62), liver (n = 28), and lung (n = 186) cancer cell lines (Figures 1A and S1). Conversely, expression of *Fzd2* and *Wnt5a*/*Wnt5b* correlated negatively with markers of epithelial cell differentiation, such as Epcam (*Epcam*), E-cadherin (*CDH1*), and keratin (*KRT18*; Figure 1A). In a panel of 48 tissue samples from patients with either liver or lung cancers, we found that *Fzd2* was significantly overexpressed in late-stage cancer (stages III and IV) relative to normal tissue and early-stage cancer (stages I and II) (HCC, $p = 0.0051$; lung, $p = 0.032$, Figure 1B). As in cell lines, levels of *Fzd2* correlated negatively with the degree of tissue differentiation—moderately and poorly differentiated tumors exhibited higher levels of *Fzd2* compared to well-differentiated tumor types (Figure S1). We therefore conclude that *Wnt5a*, *Wnt5b*, and *Fzd2* are statistically significant markers of poorly differentiated, mesenchymal-type cancer in diverse cell lines and in human tumor tissue samples.

Fzd2 Regulates Epithelial-Mesenchymal Transition and Cellular Migration

To determine whether Fzd2 signaling is required for cell growth or migration and whether Wnt5-Fzd2 signaling regulates EMT, we depleted or overexpressed Fzd2 in poorly differentiated or well-differentiated cell lines, respectively. No differences were observed in cell viability between control and RNAi-treated cells (Figure S1). However, when we assayed for cell migration using a real-time wound-healing assay, a significant reduction in closure time was observed in Fzd2-depleted cells as compared to control FOCUS (liver) and BT549 (breast) cells ($p < 0.05$; Figure 1C). Knockdown of Fzd2 also caused a decrease in cell invasion ($p < 0.05$; Figure S1). Cell lines that are poorly differentiated and express high levels of Wnt5 and Fzd2 (SNU449, SNU475, and FOCUS) migrated faster than well-differentiated lines in which ligand and receptor levels are low (HepG2 and Huh7) (Figure S1); when Fzd2 was overexpressed in cells with low or undetectable levels of endogenous Fzd2 (Huh7, liver and Dld1, colon), we observed a significant increase in cell migration compared to vector-only control ($p < 0.05$; Figure 1C). Overall, these data suggest that Fzd2 plays a causal role in cell motility.

Because Fzd2 levels correlate with mesenchymal markers in many cancer cell lines (Figure 1A), we hypothesized that Wnt5-Fzd2 signaling might drive EMT. To test this, the levels of 75 EMT-associated genes were assessed in Huh7 cells overexpressing Fzd2 (Huh7 parental cells have low levels of Fzd2) or in FOCUS cells (which are in high in Fzd2) depleted of Fzd2 by RNAi (Figures 1D and 1E). Overexpression of Fzd2 in Huh7 cells caused a significant decrease in the expression of epithelial markers such as Cdh1 (E-cadherin), Ocln (Occludin), and Keratin (Krt19), whereas expression of mesenchymal markers such as Mmp2, Mmp9, and Msn was elevated (Figures 1D and 1E). Overexpression of Fzd2 also led to increased mRNA levels of Wnt5a/b, suggesting activation of an autocrine positive feedback loop (Figure 1E). Conversely, in FOCUS cells depleted of Fzd2, mRNA levels for mesenchymal markers were reduced, including Spp1, Mmp2, Snai2 (Slug), and Mmp9, and expression of epithelial markers was elevated, including Cdh1, Ocln, and Gsc (Figure 1E). Similar results were obtained at the protein level based on reverse-phase protein arrays for E-cadherin, Occludin, MMP9, and Slug (Figure S1). Taken together, these data suggest that Fzd2 signaling drives expression of genes associated with EMT.

Fzd2-Mediated Cell Migration Is Not Dependent on Canonical Wnt Signaling or Previously Described Noncanonical Pathways

Previous studies have shown that Fzd2 can activate both β-catenin-dependent (canonical) and β-catenin-independent (noncanonical) signaling (Grumolato et al., 2010). Canonical signaling involves the transcription factor TCF, whose activity can be monitored using well-characterized TOPglow and FOPglow reporter constructs. Exposing late-stage HCC cell lines that overexpress Wnt5/Fzd2 (FOCUS, SNU449, and SNU475) to Wnt3a did not activate TCF reporter activity, but Wnt3a did activate TCF in well-differentiated HCC lines that express low levels of Wnt5/Fzd2 (HepG2 and Huh7; Figure S2). Thus, a switch appears to occur between canonical and noncanonical Wnt signaling at some stage in tumor progression. Depending on cellular context, noncanonical signaling has been shown to involve a diverse set of signaling molecules, including Rho, Rac, Rock, PI3K, CK1, PKA, PKC, JNK, mTOR, and Dvl (Figure S2). Because many of the liver cell lines in our collection proved difficult to transfect with RNAi, a pharmacological approach was used to determine whether Fzd2-mediated cell migration depends on these or other factors. Treating FOCUS cells with inhibitors of GSK3β (TDZD-8), Axin (IWR-1), β-catenin-TCF (PNU074654), β-catenin stabilization (XAV939), or any of the ten mediators of noncanonical Wnt signaling listed above did not significantly affect Fzd2-mediated cell migration ($p < 0.05$) (Figure S2). Overall, these data suggest that Fzd2-mediated promigratory signaling is not dependent on the β-catenin/TCF pathway but instead involves a previously uncharacterized, noncanonical pathway.

Discovery of a Noncanonical Signaling Pathway Downstream of Fzd2

To identify alternative pathways involved in Wnt5-Fzd2-mediated EMT and cell migration, we evaluated the basal activities of 45 reporters for different transcription factors involved in signaling pathways that have been implicated in oncogenesis in FOCUS cells expressing either Fzd2-specific shRNA (FOCUS-shFzd2) or control-shRNAs (FOCUS-shCtl) (Figure 2A and Table S1). A 10-fold reduction was observed in the activity of the Stat3 transcriptional reporter ($p < 0.001$) when Fzd2 was depleted and Elk-1- and Sp1-specific reporters were also affected to a lesser degree (Figure 2A). Exposing cells to an inhibitor of Wnt secretion (C59) decreased Stat3 transcriptional

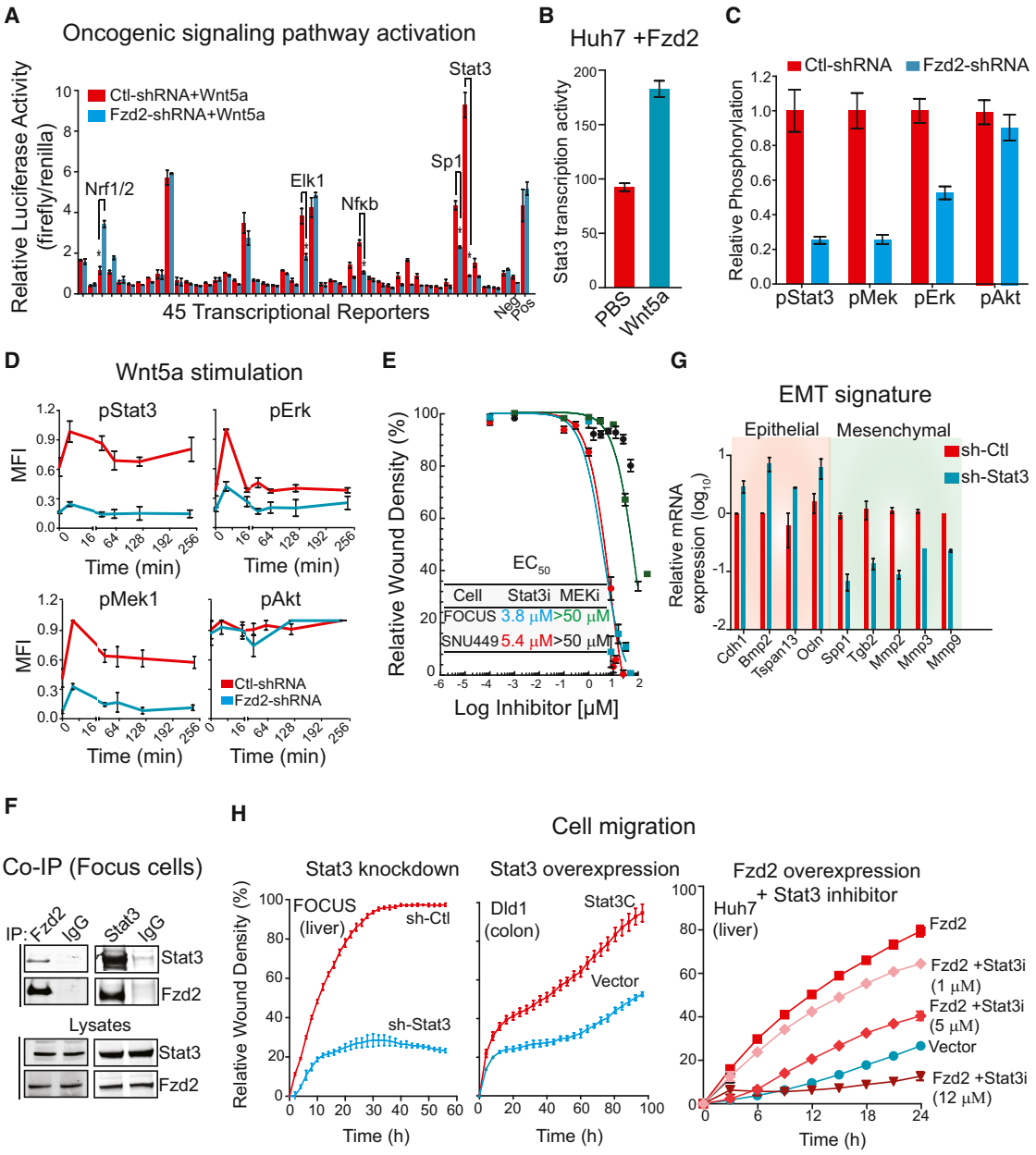

Figure 2. Stat3 Is a Key Mediator of Fzd2-Mediated Downstream Signaling, EMT Program, and Cellular Migration

(A) Comparison of 45 different signal transduction pathways in FOCUS cells transfected with Fzd2 or control shRNA using a 45-transcription factor reporter array. Signaling pathways that showed significant change in Fzd2 knockdown samples are indicated. Neg and Pos denote negative and positive luciferase controls.

(B) Bar graph showing increase in transcription activity of Stat3 upon Wnt5a stimulation in Fzd2-expressing Huh7 cells.

(C) Bar graph showing decrease in phosphorylation of Stat3, Erk1, and Mek1 upon Fzd2 knockdown in FOCUS cells. The relative phosphorylation of Akt (Ser473) is unchanged in Fzd2-shRNA-expressing cells.

(D) Wnt5a stimulation increases phosphorylation of Stat3, Erk, and Mek in a Fzd2-dependent manner.

(E) Treatment with Stat3 inhibitor reduces FOCUS cell migration. Dose response curves showing EC_{50} (50% reduction in cell migration compared with DMSO control) in FOCUS and SNU449 liver cancer cell lines treated with Stat3 or Mek inhibitors.

(F) Western blots showing that Fzd2 and Stat3 associate in a coimmunoprecipitation assay. Lysates immunoblotted with anti-Stat3 and anti-Fzd2 are also shown.

(G) Perturbing Stat3 expression reverses EMT in FOCUS cells. Bar graph shows expression of epithelial and mesenchymal marker genes in FOCUS cells with knockdown of Stat3.

(H) Stat3 activity regulates cell migration. Knocking down expression of Stat3 decreases Fzd2-mediated cell migration in FOCUS cells (left), whereas expression of constitutively active Stat3 (Stat3C) increased migration of Dld1 epithelial cells (middle). Treatment with Stattic (Stat3 inhibitor) decreased migration of Fzd2-overexpressing Huh7 cells (right) in a dose-dependent manner.

Error bars indicate SEM. See also Figures S3, S4, and S5 and Table S1.

activity in FOCUS cells 2- to 4-fold, whereas overexpressing Fzd2 in Huh7 cells increased Stat3 activity 2-fold (Figure 2B). Depletion of Fzd2 in other poorly differentiated, high Wnt5-Fzd2-expressing cell lines, including SNU449 (liver) and BT-570 (breast), decreased Stat3 transcriptional activity, whereas Elk-1 activity was not changed (Figure S3). Further, depletion of Fzd2 in FOCUS cells also decreased expression of several Stat3 target genes, including *IL2RG*, *STAM*, *PLAU*, *SerpinE1*, and *MMP3* (Figure S3). Stat3 activity is typically induced by receptor tyrosine kinases (RTKs) or by the interleukin-6 (IL-6)-Janus kinases (JAK) pathway, whereas Elk-1 is activated by the MAPK pathway (Davis et al., 2000). Consistent with these established mechanisms, phosphorylation of Stat3 ($pSer^{727}$), Mek1($pSer^{217}$/$pSer^{221}$), and Erk1 ($pThr^{202}$/Tyr^{204}) was reduced by Fzd2 depletion, but Akt phosphorylation ($pSer^{473}$) and the transcriptional activity of FOXO (which lies downstream of the Akt pathway) was unaffected (Figures 2C and S3). When cells were exposed to exogenous Wnt5a, Fzd2-dependent phosphorylation of Stat3, Mek1/2, and Erk1/2 (but not Akt) was observed (Figure 2D).

Small-molecule inhibitors were used to investigate whether the Stat3 and/or MAPK pathways, both of which have documented roles in cell migration (Tarcic et al., 2012; Teng et al., 2009), play a causal role in Fzd2-mediated migration in liver, lung, and breast cancer cell lines (Figures 2E and S3). Despite its low potency, the Stat3 inhibitor Stattic (IC_{50} ~5 μM) (Schust et al., 2006) decreased migration in cell lines expressing high levels of Fzd2; inhibition was observed in the low micromolar range. In contrast, even the relatively potent MEK inhibitor U0126 (IC_{50} ~70 nM) (Duncia et al., 1998) had no effect on cell migration in six cell lines tested (Figures 2E and S3). Although it is plausible that Ras-ERK signaling can contribute to EMT or other aspects of tumor progression, we conclude that Stat3, rather than MAPK/Elk-1, is more likely to play a causal role in Fzd2-mediated cell migration.

Stat3 Interacts with Fzd2 and Plays a Critical Role in Wnt5-Fzd2-Mediated EMT and Cell Migration

Stat3 is phosphorylated on Tyr^{705} or Ser^{727}, two sites required for maximal transcriptional activity in response to cytokines (Wen et al., 1995). To determine which Stat3 phosphorylation sites are involved in Wnt5-Fzd2 signaling, we overexpressed a wild-type or a constitutively active mutant, Stat3-C (Takahashi and Yamanaka, 2006). This resulted in 2-fold and 4-fold increases in Stat3 transcriptional activity, respectively (Figure S3). Overexpression of Stat3-S727A (Wen and Darnell, 1997) also increased transcription 2-fold in FOCUS cells, similar to wild-type Stat3. In contrast, overexpression of Stat3-Y705F (Wen and Darnell, 1997) was indistinguishable from vector-only control. These data suggest that Stat3-$pTyr^{705}$ is involved in Fzd2-mediated signaling. In addition, we found that endogenously expressed Fzd2 and Stat3 coimmunoprecipitated reciprocally in four different cancer cell lines (FOCUS, BT549, Calu1, and NCIH661) (Figures 2F and S3). A pull-down assay using a GST-Stat3 fusion protein, however, failed to recover Fzd2 from FOCUS cell lysates, suggesting that the interaction may be indirect (Figure S3). Stat3 depletion reduced the expression of mesenchymal markers such as Spp1, Mmp2, Snai2 (Slug), and Mmp9 and enhanced expression of epithelial markers such as Cdh1 and Ocln (Figure 2G), whereas overexpression of constitutively active mutant (Stat3-C) in Huh7 epithelial cells decreased expression of epithelial markers such as Cdh1, Krt19, and Ocln and increased levels of Vimentin (Figure S3). Similar changes were observed in cells treated with a pharmacological inhibitor of Stat3 and were dose- and time-dependent (Figure S3). As further confirmation, knocking down Stat3 by RNAi impaired wound closure in FOCUS cells, whereas overexpression of constitutively active Stat3 increased cell migration in Dld1 colorectal cancer cells, which have low levels of Fzd2 (Figure 2H). Finally, pharmacological inhibition of Stat3 in Fzd2-expressing Huh7 cells abolished cell migration in a dose-dependent manner (Figure 2H). We conclude that Fzd2-dependent EMT and cell migration involves Stat3 activation and that this likely involves phosphorylation of Stat3 on Tyr^{705}. Moreover, Fzd2 and Stat3 physically associate, most likely in a complex involving additional proteins.

Fzd2 Mediates Stat3 Activation and Cell Migration Independent of Janus Kinases

Although Stat3 is phosphorylated on Tyr^{705} in a Wnt5–Fzd2-dependent manner (Figure S3), Fzd2 is a member of the G-protein-coupled family of receptors and therefore lacks tyrosine kinase activity. Treating FOCUS cells with any of three well-characterized inhibitors of αβγ-trimeric G proteins (pertussis toxin, Gallein, and Suramin) (Freissmuth et al., 1996; Katada, 2012) had no effect on cell migration or Stat3 reporter activity (Figure S4), suggesting that activation of a heterotrimeric G protein is not involved. We therefore searched for a kinase involved in Fzd2-mediated phosphorylation of Stat3. JAKs phosphorylate and activate Stat3 in response to cytokines (O'Shea et al., 2002), and Stat3 activation by IL-6 in FOCUS or SNU449 (by ~2- to 4-fold ; Figure S4) was blocked by ruxolitinib, a JAK1/2 inhibitor (Harrison et al., 2012), or tofacitinib, a pan-JAK inhibitor (Paul and Roblin, 2012; EC_{50} < 1 nM; Figure S4). However, JAK inhibition had little or no effect on Wnt5a-induced Stat3 transcription in either FOCUS or SNU449 cells except at drug concentrations so high that selectivity is lost (EC_{50} > 15 μM; Figure S4). These data show that Janus kinases are required for IL-6-, but not Wnt5a–Fzd2-mediated activation of Stat3.

To determine whether Fzd2 cross-activates an RTK that subsequently phosphorylates Stat3, we used antibody microarrays to monitor the tyrosine phosphorylation states of 40 RTKs and 12 downstream signaling kinases in FOCUS cells expressing either Fzd2-specific or control shRNA (Figure S5). Previously established differences in the phosphorylation levels of Stat3 and Akt (Figures 2C and 2D) were used as positive and negative controls, respectively. No significant differences were observed for 38 of 40 RTKs examined, including ROR1, ROR2, and RYK, all three of which have been shown to interact with Fzd2 and Wnt5a (Li et al., 2008; Lin et al., 2010) (Figure S5). Tyrosine phosphorylation of EGFR and c-Met, however, was reduced >2-fold ($p < 0.05$) in FOCUS-shFzd2 compared to FOCUS-shCtl cells. Quantitative western blotting confirmed these findings and revealed that protein levels of these two receptors were reduced by Fzd2 knockdown, as were transcript levels as determined by qPCR (Figure S5). Despite these effects, stimulation with either

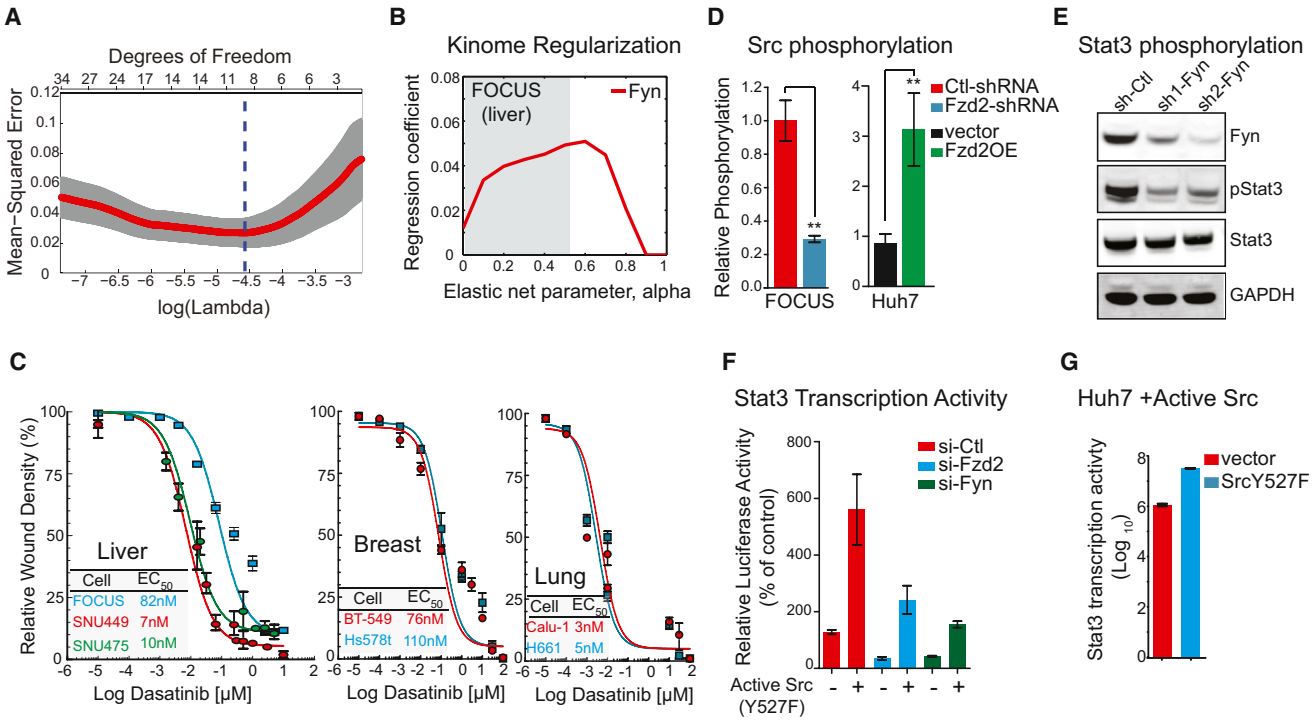

Figure 3. Fyn Kinase Is a Critical Regulator of Fzd2-Mediated Stat3 Activity

(A) Identification of informative kinases in Fzd2-mediated cell migration using kinome regularization. Plot shows LOOCV error using elastic net regularization fit. The error bars represent cross-validation error plus 1 SD. The kinases identified at absolute minima (blue dashed line) were termed the most informative kinases.

(B) Evolution of regression coefficients. Plot showing regression coefficients for Fyn kinase against value of elastic-net penalty α. Nonzero regression coefficients for kinases picked at $\alpha > 0.5$ (gray region) are considered significantly informative.

(C) Src family kinase inhibitor reduces Fzd2-mediated cellular migration. Relative wound density of cancer cells treated with varying concentration of Dasatinib was monitored for 96 hr. Dose-response curves of Dasatinib treatment in seven cancer cell lines and respective EC_{50} are shown.

(D) Knockdown of Fzd2 expression reduces phosphorylation of SFKs in FOCUS cells, whereas overexpression of Fzd2 increases Src phosphorylation in Huh7 cells.

(E) Fyn kinase phosphorylates Stat3. Western blots showing phosphorylation of Stat3 upon knockdown of Fyn in FOCUS cells.

(F) Wnt5-Fzd2-dependent Stat3 transcription activity can be rescued by overexpression of active Src in Fzd2 or Fyn knockdown cells.

(G) Overexpression of active SFK (SrcY527F) in Huh7 cells increased transcriptional activity of Stat3.

Error bars indicate SEM. See also Figure S6.

EGF or HGF or inhibition with EGFR family kinase inhibitors (Lapatinib, Erlotinib, and Gefitinib) or c-Met kinase inhibitors (SU11274 and Crizotinib) had no observable effect on either cell migration or Stat3 activity at reasonable drug concentrations (<10 μM, Figure S5). We conclude that Fzd2 may cross-regulate EGFR and c-Met, but neither receptor plays a causal role in Wnt5-mediated cell migration.

Kinome Regularization Identifies Fyn Kinase as a Key Mediator of Fzd2 Signaling and Cellular Migration

Having eliminated two obvious candidates for the Stat3 kinase, we used a recently established unbiased method of target deconvolution, kinome regularization (KR), which exploits the polypharmacology of kinase inhibitors (Gujral et al., 2014). In this method, LASSO, a multivariate regression technique, was used to regress a single target variable (quantified cell migration) against a set of second variables (the activities of individual kinases assayed in vitro at 500 nM) while imposing a penalty that eliminates poorly correlated variables (kinases with insignificant contributions). Leave-one-out cross-validation using least-mean-square error implicated a panel of 16 kinases in phosphorylating Stat3 in FOCUS cells (Figure 3A). Of these, eight were tyrosine kinases, and Fyn in particular was identified as an "informative kinase" in both FOCUS and Hs578t cells (Figures 3B and S6). The pan-specific Src family kinase (SFK) inhibitor Dasatinib reduced cell migration not only in FOCUS cells but also in other high Fzd2-expressing cell lines, including HCC (SNU449 and SNU475), breast (BT-549 and Hs578t), and lung (Calu-1 and NCI-H661) with EC_{50} values of 3–100 nM (Figure 3C). SFK phosphorylation was reduced ~3-fold in FOCUS-shFzd2 cells as compared to FOCUS-shCtl cells, whereas it was increased ~3-fold in Fzd2-expressing Huh7 cells compared to vector-only-expressing Huh7 epithelial cells, as assayed using an antibody that recognizes a conserved site of tyrosine phosphorylation present on all SFKs and corresponding to Tyr^{416} in Src (Figures 3D and S6). Consistently, phosphorylation of Fyn-Tyr^{420} was also reduced by 2-fold in FOCUS-shFzd2 cells as compared to FOCUS-shCtl cells (Figure S6). Knockdown of

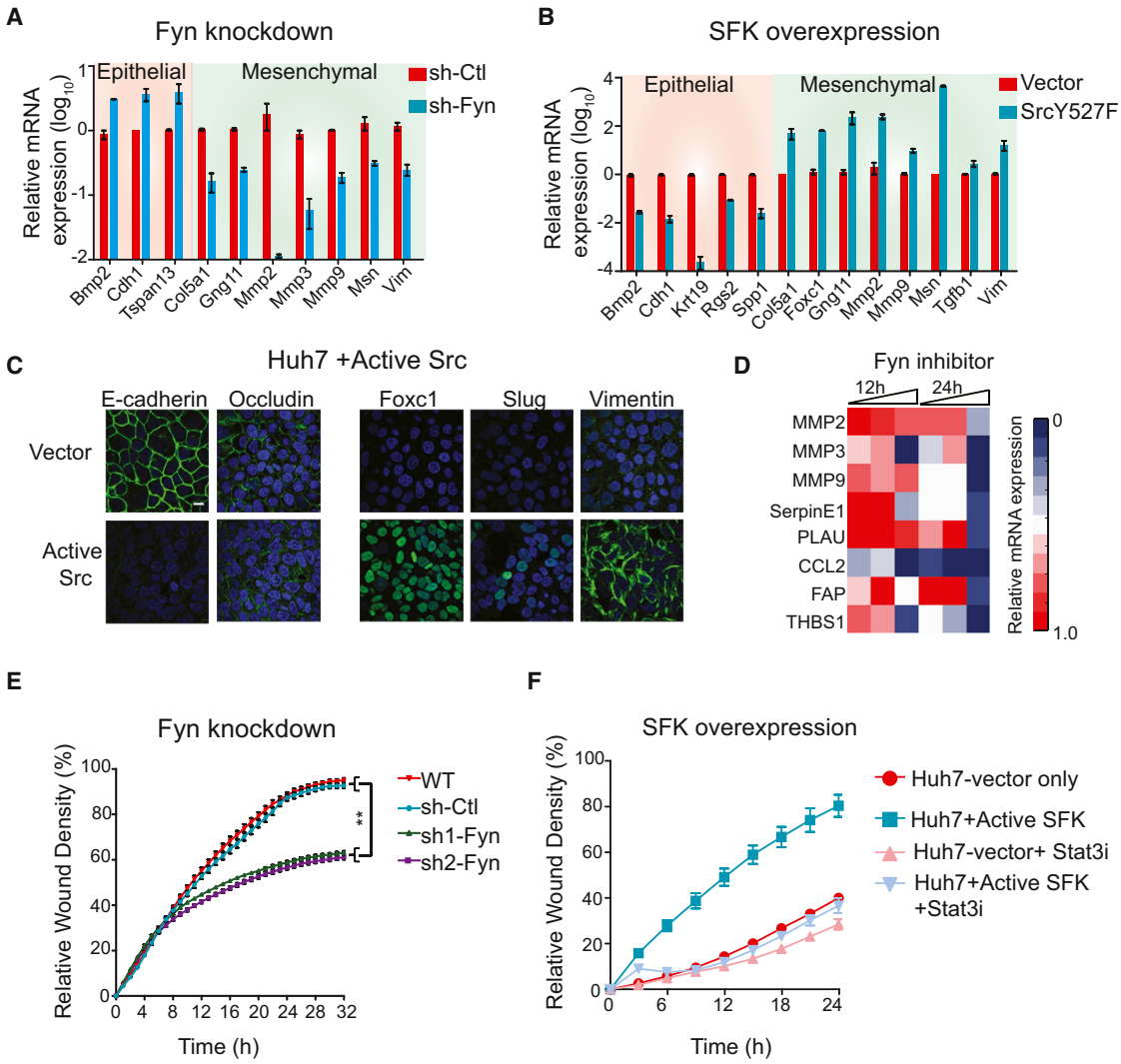

Figure 4. Fyn Regulates Fzd2-Mediated EMT Program and Cellular Migration

(A and B) (A) Perturbing Fzd2-dependent Fyn activity reverses EMT. Plots showing mRNA expression of selected EMT genes measured by qPCR in FOCUS cells expressing shRNA against Fyn or (B) Huh7 cells expressing active Src (Src Y527F).

(C) Representative images showing expression of active Src in Huh7 cells decreased levels of epithelial markers, E-cadherin, and Occludin and increased levels of mesenchymal markers, Foxc1, Slug, and Vimentin. Blue nucleus stain. Scale bar, 100 pixels.

(D) Heat map showing effect of Fyn inhibitor (Dasatinib) on expression of EMT-associated genes.

(E and F) Fyn-shRNA showed significant decrease in Fzd2-mediated cell migration in FOCUS cells, whereas expression of SrcY527F increases cell migration in Huh7 cells. Treatment with Stattic (Stat3 inhibitor) decreased migration of Huh7 cells expressing SrcY527F to the wild-type Huh7 levels.

Error bars indicate SEM. See also Figure S6.

Fyn also inhibited Stat3-Tyr^{705} phosphorylation and transcriptional activity, suggesting that Fyn kinase lies upstream of Stat3 (Figures 3E and 3F). We note, however, that Stat3 activity can also be induced >6-fold by overexpressing a constitutively active form of Src (Src-Y527F) in FOCUS cells (Figure 3F) or Huh7 cells (Figure 3G) or in FOCUS cells depleted of either Fzd2 or Fyn, suggesting that SFK members may be functionally redundant (Figure 3F).

Next, we assessed whether Fyn also plays a role in Fzd2-mediated regulation of EMT. RNAi-mediated depletion of Fyn in FOCUS cells reduced expression of the mesenchymal markers Mmp2, Snai2, and Mmp9, whereas expression of epithelial markers was elevated, including Cdh1, Bmp2, and Tspan13 (as assayed at the mRNA level Figure 4A). Consistently, expression of functionally redundant active SFK in Huh7 epithelial cells decreased expression of epithelial markers (Bmp2, Cdh1, and Krt19), whereas expression of mesenchymal markers (Mmp2, Mmp9, Vim, Foxc1, Slug, Msn, and Tgfb1) was significantly increased, suggesting that Fyn is a critical regulator of EMT (Figures 4B and 4C). Similar results were obtained in FOCUS cells treated with the Fyn inhibitor Dasatinib, and changes in expression were dose- and time-dependent

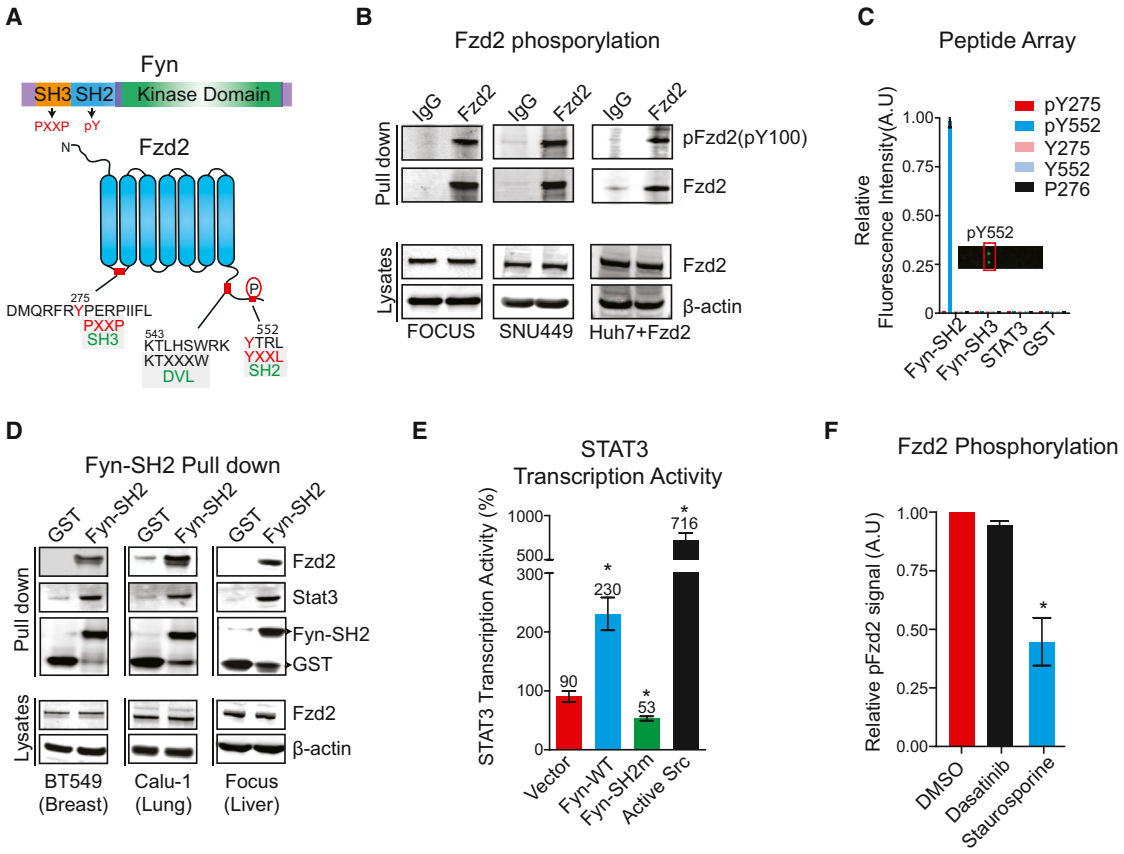

Figure 5. Fzd2 Is Tyrosine Phosphorylated and Is Directly Associated with the Fyn-SH2 Domain

(A) Schematics showing domain structures of Fyn-kinase and Fzd2 proteins. Fyn contains an SH3 domain, SH2 domain, and a kinase domain. Fzd2 is a seven transmembrane domain-containing protein. Tyrosine residues in the first cytosolic loop (Y^{275}) and in the C-terminal tail (Y^{552}) are highlighted. Dvl-binding sequence in the C-terminal domain of Fzd2 is also shown.

(B) Fzd2 is tyrosine phosphorylated in three HCC cell lines. Western blots showing tyrosine phosphorylation of Fzd2 detected by immunoblotting with anti-phosphotyrosine antibody (pY100) in immunoprecipitates. Total protein levels of Fzd2 and β-actin in whole-cell lysates are also shown.

(C) Fzd2-pY^{552} binds directly to the SH2 domain of Fyn. A peptide array consisting of phosphorylated tyrosine 275 (pY^{275}), pY^{552}, nonphosphorylated tyrosine 275 (Y^{275}), Y^{552} and a peptide containing proline-rich region from the first cytoplasmic loop of Fzd2 (P^{276}) were incubated with purified SH2 domain of Fyn, SH3 domain of Fyn, and purified Stat3 of GST control proteins. Protein-peptide interaction was measured by probing arrays with anti-GST antibody. A plot of relative fluorescence intensity measured on the array is shown.

(D) Western blots showing GST pull-down of Fzd2 and Stat3 using purified SH2 domain of Fyn. The pull-downs were subjected to western blotting and immunoblotted with anti-Fzd2, Stat3, and GST antibodies. Total protein levels of Fzd2 and β-actin in whole-cell lysates are also shown.

(E) SH2 domain of Fyn is critical for Wnt5/Fzd2-mediated Stat3 transcriptional activity. Stat3 transcriptional activity was measured in FOCUS cells transfected with the indicated constructs.

(F) A bar graph showing Fzd2 tyrosine phosphorylation in FOCUS cells treated with DMSO, Dasatinib (1 μM), or Staurosporine (100 nM) for 30 min. Fzd2 phosphorylation was detected by immunoblotting with anti-phosphotyrosine antibody (pY100) in Fzd2 immunoprecipitates. Data are the mean of at least two independent samples, and error bars indicate SEM.

Error bars indicate SEM. See also Figure S6.

(Figure 4D). Depleting Fyn reduced the ability of FOCUS cells to migrate in a wound-healing assay (Figure 4E), whereas expression of functionally redundant active SFK significantly increased migration of Huh7 cells ($p < 0.05$) (Figure 4F). Interestingly, inhibition of Stat3 activity in Huh7 cells expressing active Src decreased migration to wild-type Huh7 levels, suggesting that Stat3 activity is important for SFK-mediated cell migration (Figure 4F). We conclude that Fzd2 mediates EMT and cell migration through Fyn-dependent activation of Stat3.

Fzd2 Is Tyrosine Phosphorylated and Directly Associates with the SH2 Domain of Fyn

Fyn has the canonical architecture of a SFK, including an N-terminal Src homology 3 (SH3) domain, followed by a Src homology 2 (SH2) domain, a tyrosine kinase domain, and a short C-terminal tail (Figure 5A) (Lenaerts et al., 2008). SH3 domains bind to proline-rich motifs, whereas SH2 domains recognize sites of tyrosine phosphorylation. Based on our current understanding of SFKs, the potential binding of Fyn to Fzd2 could involve either its SH2 or SH3 domain. Immunoprecipitation

of Fzd2 and immunoblotting with a pan-specific anti-phosphotyrosine antibody (pY100) revealed that Fzd2 is tyrosine phosphorylated in both FOCUS and SNU449 cells, as well as in Wnt5a-induced Fzd2-expressing Huh7 cells (Figure 5B). Fzd2 contains two tyrosine residues that could potentially be phosphorylated: Tyr^{275} in the first cytoplasmic loop and Tyr^{552} in the C-terminal tail. It also has a single proline-rich region in its first cytoplasmic loop (the sequence ^{276}PERP^{279}). To determine whether Fyn can bind either of the two phosphotyrosine sites, we prepared a peptide array comprising phosphorylated and unphosphorylated 18-mer peptides containing Tyr^{275} or Tyr^{552} of Fzd2, as well as a peptide containing the PERP motif. We probed the array with purified recombinant Fyn-SH2, Fyn-SH3, and Stat3 (Figure 5C). Glutathione-*S*-transferase (GST) was used as a negative control. The SH2 domain of Fyn bound the pTyr552 peptide (Figure 5C), but neither the SH2 nor SH3 domains bound appreciably to the nonphosphorylated or PXXP-containing peptides. Surface plasmon resonance measurements showed that the SH2 domain of Fyn bound to the pTyr552 peptide with an affinity (K_D = 2.1 nM; Table S3) consistent with previously reported SH2 domain-peptide interactions by Src family members (Payne et al., 1993). None of the Fzd2-derived peptides bound recombinant Stat3, which is consistent with our hypothesis that the interaction between Fzd2 and Stat3 is indirect. To determine whether the SH2 domain of Fyn can interact with full-length Fzd2 in a cellular environment, we performed a pull-down experiment using recombinant GST-FynSH2 and lysates obtained from BT549, Calu-1, or FOCUS cell lines. In all three cases, we detected Fzd2 binding to GST-FynSH2, but not to GST alone (Figure 5D). We also detected Stat3 in these pull-downs, which is consistent with formation of a multiprotein complex that includes Fzd2, Fyn, Stat3, and possibly other proteins as well.

To determine whether the SH2 domain of Fyn is required for Stat3 activation by Fzd2, we generated an SH2 domain mutant, Fyn-R176E, that is predicted to fold correctly but have substantially lower affinity for tyrosine phosphorylated target peptides (Mariotti et al., 2001). When overexpressed in FOCUS cells, wild-type Fyn and constitutively active Src-Y527F increased Stat3 activity 2- to 7-fold, respectively, whereas overexpression of Fyn-R176E decreased Stat3 activity 2-fold, implying that Fyn-R176E has dominant-negative activity (Figure 5E). These data suggest that the SH2 domain of Fyn is involved in Wnt5-Fzd2-mediated Stat3 activation. To determine whether Fyn is the kinase responsible for phosphorylation of Fzd2, we treated cells with sufficient Dasatinib to block Fyn autophosphorylation at Tyr^{420} but did not observe a detectable reduction in Fzd2 phosphorylation (Figures 5F and S6). As a positive control, we confirmed that phosphorylation of Fzd2 was substantially decreased when cells were treated with Staurosporine, a broad-spectrum kinase inhibitor (Figure 5F). We conclude that Fzd2 is tyrosine phosphorylated on Tyr^{552} by an as-yet-unidentified kinase, that this promotes binding of Fzd2 to the SH2 domain of Fyn kinase, and that this in turn activates Stat3 via phosphorylation of Tyr^{705}. These signal transduction events appear to involve the formation of a multiprotein complex among Fzd2, Stat3, Fyn, and possibly other proteins.

Fzd2 Knockdown or Treatment with an Anti-Fzd2 Antibody Reduces Tumor Growth and Metastasis in a Mouse Xenograft

To assess the role played by Fzd2 in tumorigenesis, we used a model in which FOCUS or Huh7 cells were injected subcutaneously into athymic mice. FOCUS cells grew rapidly in this xenograft model, producing palpable tumors by day four. When the tumors were ~200 mm^3 (as measured using a caliper), mice were randomized into treatment and control groups. The former received subcutaneous Fzd2-siRNA injections on alternate days for 2 weeks, and the latter received transfection reagent alone. We observed that tumor growth was significantly slower in the treatment group compared to the control group, with a noticeable lag in the exponential growth phase (Figure 6A). Notably, tumor growth resumed when Fzd2-siRNA injections were discontinued.

As a first step in developing a potential anti-Fzd2 therapeutic, we generated and characterized Fzd2-specific neutralizing antibodies in rats (Figures S6 and S7). We discovered an isotype-specific epitope on Fzd2 (spanning residues Glu^{134}-Leu^{163} in the cysteine rich and juxtamembrane domains) for which cognate antibodies cause receptor internalization and inhibition of downstream signaling (Figures S6 and S7). Targeting Fzd2 specifically with two different antibodies that recognize this region reduced Stat3 transcription activity and tumor cell migration and invasion in vitro (Figure S7). These antibodies had no effect on Wnt3a-induced activation of TCF activity. We tested the effects of monoclonal anti-Fzd2 antibodies that cause Fzd2 internalization and degradation on tumor volume and metastasis (Figure 6). Athymic mice were subcutaneously injected with FOCUS-Luc cells and randomized into three groups that received either vehicle control, a low antibody dose (10 mg/kg Fzd2 mAb, q3d), or a high antibody dose (30 mg/kg Fzd2 mAb, q3d). Injection of anti-Fzd2 antibody caused a significant dose-dependent decrease in tumor growth for two different antibodies ($p < 0.05$; Figure 6B). No weight loss or other obvious adverse effects were observed. When liver and lung tissue were recovered from mice treated with one of the anti-Fzd2 antibodies, 1 of 12 mice was observed to have metastases. In contrast, 12 of 16 control mice had metastases to either liver or lung (Figure 6C). Consistently, mice injected with Huh7 cells overexpressing Fzd2 showed no change in tumor growth but significantly higher incidence of metastasis (nine of nine) than mice injected with Huh7-vector-only-expressing cells (four of eight) (Figures 6C and 6D). These data show that downregulating Fzd2 signaling by antibody treatment attenuates Fzd2-mediated tumor growth and metastasis, implying that Fzd2 may serve as a new drug target for late stage HCC. Moreover, high expression of Fzd2 and/or Wnt5a/b may serve as a biomarker for potentially responsive tumors.

Finally, we asked whether elevated expression of Wnt5, Fzd2, and a set of 31 genes regulated by the Fzd2-Fyn-Stat3 pathway (dubbed the "Fzd2 signature") could be used as a predictive marker of metastasis and decreased overall survival in HCC patients (Ye et al., 2003). This was accomplished using ADT (alternating decision tree) analysis that generates trees in which the contribution of each gene can be visualized. The Fzd2

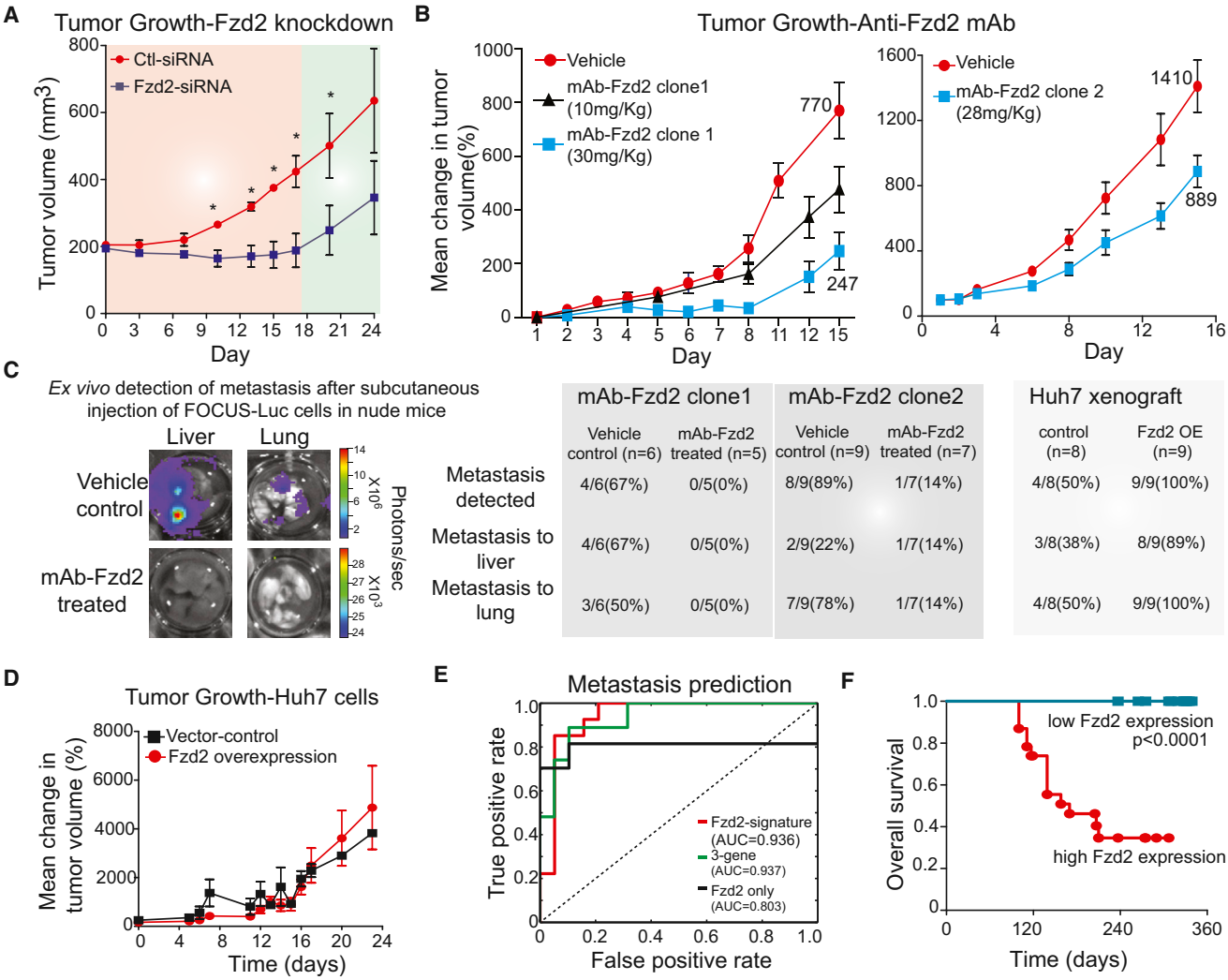

Figure 6. Fzd2 Knockdown or Treatment with an Anti-Fzd2 Antibody Reduces Tumor Growth and Metastasis in Mouse Xenograft

(A) Knockdown of Fzd2 expression reduces tumor growth in nude mice. FOCUS cells were injected s.c. into athymic mice and the ability of cells to form tumor outgrowths was monitored in the presence (red shade) or absence (green shade) of siRNA against Fzd2.

(B) Treatment with two different clones of anti-Fzd2 antibodies reduced tumor growth in nude mice in a dose-dependent manner. Athymic mice were subcutaneously injected with FOCUS-Luc cells. When the outgrowths were ~200 mm^3, mice were divided at random into three groups (vehicle control, mAb-Fzd2 10 mg/kg, and mAb-Fzd2 30 mg/kg) for clone1 and into two groups (vehicle control and mAb-Fzd2 30 mg/kg) for clone 2 treatment. The treated group received mAb-Fzd2 injection twice a week for 2 weeks, whereas the control group received s.c injection of vehicle.

(C) Ex vivo detection of metastasis after subcutaneous injection of FOCUS-luc or Huh7-Luc cells in nude mice. Liver and lungs were dissected from mice treated with 30 mg/kg antibody clone 1 or 28 mg/kg antibody clone 2 as well as the vehicle-treated control group to examine metastasis. Liver and lungs were dissected from mice injected with Huh7 cells expressing Fzd2 or vector only controls.

(D) Overexpression of Fzd2 expression in Huh7 cells does not affect tumor growth in nude mice. Huh7 cells transfected with either empty vector or vector encoding Fzd2 gene were injected s.c. into athymic mice, and the ability of cells to form tumor outgrowths was monitored.

(E) A Fzd2-gene signature (55 genes), 3-gene signature (Fzd2, E-cadherin, and MMP9), and Fzd2-only correctly predicted metastasis in 46 cases of HCC. AUC represent area under the curve.

(F) Kaplan-Meier survival curves for 46 HCC patients. The statistical p value was generated by the Cox-Mantel log-rank test.

Error bars indicate SEM. See also Figure S7 and Table S2.

signature, or expression of Fzd2 alone, allowed us to predict metastasis with 89% and 85% accuracy, respectively, in a group of 46 HCC patients (Figure S7). Moreover, a signature comprising three genes—Fzd2, CDH1, and MMP9—was as accurate in predicting metastasis (89%) as the 55-gene signature (Figures 6E and S7 and Table S2). HCC patients with tumors that express high levels of Fzd2 had significantly poorer survival ($p < 0.0001$) than patients with low Fzd2 expression (Figure 6F), and Fzd2 expression was predictive of survival in a polynomial model evaluated by cross-validation (Figure S7). We conclude

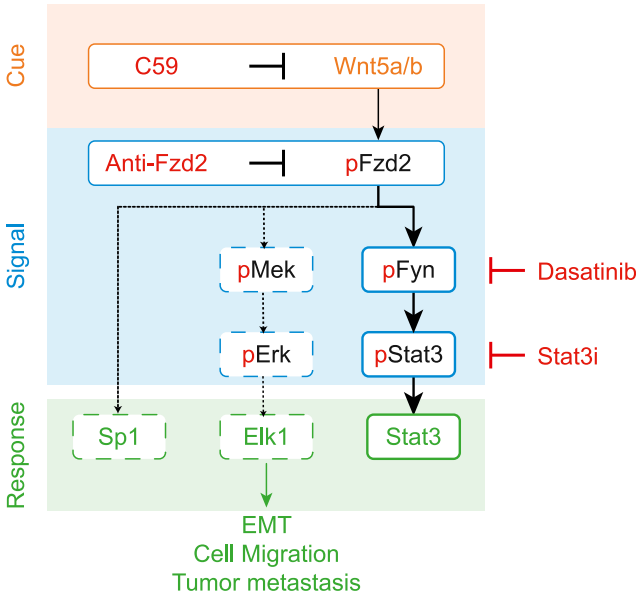

Figure 7. A Schematic of a Noncanonical Fzd2 Pathway
Wnt5-Fzd2-Fyn-Stat3 axis contributes to EMT program, cellular migration, and tumor metastasis. Dashed line indicates the provisional nature of this pathway.

that high expression of Fzd2 is a potential marker of poor clinical outcome in HCC patients.

DISCUSSION

Metastasis is responsible for as much as 90% of cancer-associated mortality (Weigelt et al., 2005). Regrettably, progress in developing effective drugs specifically targeting metastasis or cells with metastatic potential has been slow (Sleeman and Steeg, 2010). Our study provides evidence that activation of Fzd2-mediated signaling may be important in several metastatic, late-stage cancers. We found that Fzd2 and its cognate ligands Wnt5a and Wnt5b are overexpressed in metastatic cancer cell lines and tumors. This pattern of expression appears to drive an autocrine loop that leads to expression of markers of EMT and increased cell migration. Overall, our in vitro and in vivo data suggest that Fzd2 is an oncogene and that overexpression of Fzd2 and signaling via a noncanonical Wnt pathway contributes to the progression of late-stage metastatic cancers (Figure 7).

Although there are numerous studies showing the migratory potential of metastatic cells and relating metastasis to the biology of the epithelial-mesenchymal transition, little is known about how tumor cells access this fundamental cellular program. In the case of Fzd2, we found that Wnt5 activation induces cell migration via a noncanonical Wnt signaling pathway that involves the tyrosine kinase Fyn and the transcription factor Stat3. Stat3 is well known to mediate cytokine signaling and to elicit a variety of inflammatory responses. Recently, RTK or Oncostatin M-mediated activation of Stat3 was shown to contribute to EMT through comprehensive alterations of transcription factors such as Zeb1 (Balanis et al., 2013; Guo et al., 2013). Our study, in multiple Wnt5-Fzd2-expressing tumor cells, shows an unconventional mechanism of Stat3 activation that drives EMT, cellular migration, and invasion.

The interaction of Fzd2 with Stat3 leads to Stat3 phosphorylation, but the mechanism of this activation is puzzling, as Fzd2 is not known to be a kinase. We therefore looked for an intervening kinase. We used a variety of systematic pathway mapping tools, including panels of transcriptional reporters and protein arrays, to identify the putative Stat3 kinase that lay downstream of Fzd2. The most powerful approach was a newly developed statistical machine learning tool, KR, which can deconvolve the polypharmacology of a panel of kinase inhibitors with complex and overlapping selectivities against the raw phenotype of cell migration. Combined with expression data in cell lines, the KR approach identified the tyrosine kinase Fyn as the key mediator of Fzd2-driven Stat3 phosphorylation. We then confirmed that activated Fzd2 is tyrosine phosphorylated and that Fyn associates with Fzd2-Tyr^{552} through its SH2 domain. What still remains unknown in this pathway is the kinase responsible for the initial phosphorylation of Fzd2, which is required for mediating the Fzd2-Fyn interaction. This activated complex can recruit and phosphorylate Stat3 on Tyr^{705} and appears to drives a transcriptional program that converts an epithelial morphology to a migratory mesenchymal one. Perturbation of Fzd2 signaling also affects the levels of other growth factors known to regulate EMT, such as Tgfb2 and Bmp2, suggesting that this pathway may be a master regulator of EMT, a process important in cancer and embryonic development. These studies make more concrete the general expectation that GPCRs and Src family kinases are intimately involved in multilayered forms of crosstalk that influence many cellular processes (Luttrell and Luttrell, 2004).

An understanding of this new noncanonical pathway downstream of Fzd2 may be important not only in the initiation of metastasis but in chemoresistance. RTK-mediated signaling pathways share multiple downstream signaling elements, and inhibiting the dominant RTK often results in the compensatory recruitment of downstream components by other RTKs, an important mechanism of chemoresistance (Wilson et al., 2012). Signaling through Fyn (or other Src family kinases) and Stat3 is canonically activated by RTKs such as EGFR and c-Met. Our discovery of Fzd2-mediated activation the Fyn-Stat3 axis may represent a resistance mechanism by which cancer cells could sustain proliferative signal independent of RTKs.

The gene signature regulated by the Wnt5/Fzd2 pathway seems to have strong predictive value for metastasis and overall patient survival; retrospective analysis of human tumors shows that the survival of patients with HCC overexpressing Fzd2 is substantially worse than for patients with tumors that exhibit low Fzd2 expression. Many of the intracellular proteins (pStat3, pSrc, pMek, and pErk) that are regulated by autocrine Wnt5-Fzd2 signaling could also be used as potential pharmacodynamic markers of drug response. The importance of extracellular control of EMT through Fzd2 is enhanced by our discovery of an isotype-specific epitope on Fzd2 for which we developed an antibody that is able to mediate receptor internalization and inhibition of downstream signaling. When we targeted Fzd2 specifically with such an antibody, it reduced tumor cell

migration and invasion in vitro and inhibited tumor growth and metastasis in mouse xenografts. However, whether the reduction in metastasis observed in the xenograft model is a consequence of reduced dissemination, reduced survival in the circulation, reduced extravasation, or prolonged dormancy remains to be determined. Treatment with an anti-Fzd2 antibody might therefore prove effective in the treatment of aggressive HCC and other Wnt5/Fzd2-driven tumors. Furthermore, detailed knowledge of a pathway that drives migration allows us to consider codrugging strategies involving anti-Fzd2 antibodies and existing small-molecule kinase inhibitors that target SFKs (such as Dasatinib and Bosutinib). Our understanding of the signaling cascade downstream of Fzd2 affords an opportunity for the rational design of combination regimens based on anti-Fzd2 therapy.

EXPERIMENTAL PROCEDURES

Cell Lines and Reagents

Cancer cell lines SNU449, SNU475, BT549, Hs578t, Calu-1, NCIH661, and HepG2 cells were obtained from American Type Culture Collection (ATCC, Rockville). FOCUS and Huh7 cells were obtained from J. Wands (Brown University) and have been described previously (He et al., 1984). All cell lines were maintained in Dulbecco's modified Eagle medium (DMEM) supplemented with 10% (v/v) fetal bovine serum (FBS), 2 mM glutamine, 100 IU/ml penicillin, and 100 μg/ml streptomycin.

Kinetic Wound-Healing Assay

The effect of Fzd2 knockdown on migration of FOCUS cells was studied using a wound-healing assay. FOCUS cells were plated on 96-well plates (Essen ImageLock, Essen Instruments), and a wound was scratched with wound scratcher (Essen Instruments). Small-molecule inhibitors at different doses were added immediately after wound scratching, and wound confluence was monitored with Incucyte Live-Cell Imaging System and software (Essen Instruments). Wound closure was observed every hr for 48–96 hr by comparing the mean relative wound density of at least four biological replicates in each experiment.

Tumorigenicity in Nude Mice

All in vivo experiments were performed using 6-week-old to 8-week-old athymic nude mice. Mice were maintained in laminar flow rooms with constant temperature and humidity. FOCUS cells were inoculated subcutaneously (s.c.) into each flank of the mice. Cells (2×10^6 in suspension) were injected on day 0, and tumor growth was followed every 2 to 3 days by tumor diameter measurements using vernier calipers. Tumor volumes (V) were calculated using the formula: $V = AB^2/2$ (A, axial diameter; B, rotational diameter). When the outgrowths were ~200 mm^3, mice were divided at random into two groups (control and treated). The treated group received Fzd2-siRNA injection or anti-Fzd2 antibody on alternate days (MWF) for 2 weeks, whereas the control group received s.c. injection of in vivo transfection reagent only or control IgG.

SUPPLEMENTAL INFORMATION

Supplemental Information includes Extended Experimental Procedures, seven figures, and two tables and can be found with this article online at http://dx.doi.org/10.1016/j.cell.2014.10.032.

AUTHOR CONTRIBUTIONS

T.S.G., M.C., and G.M. conceived, directed, designed, and interpreted results and wrote the manuscript. T.S.G. and M.C. designed and performed experiments. M.W.K. helped to design and interpret results and write the manuscript. P.K.S. interpreted results and helped to write the manuscript. L.P. performed kinome regularization and statistical analyses.

ACKNOWLEDGMENTS

This study was supported by awards from the National Institutes of Health (R01 GM072872, P50 GM68762, U54 HG006097, R01 HD073104, and R01 GM103785). T.S.G. is a Human Frontier Science Program Fellow. We thank the staff of the Nikon Imaging Center and Systems Biology Flow Cytometry Facility at Harvard Medical School for help and support. G.M. is an employee, cofounder, and shareholder of Merrimack Pharmaceuticals and P.K.S. is a cofounder and shareholder of Merrimack Pharmaceuticals.

Received: June 15, 2014
Revised: August 25, 2014
Accepted: October 20, 2014
Published: November 6, 2014

REFERENCES

Balanis, N., Wendt, M.K., Schiemann, B.J., Wang, Z., Schiemann, W.P., and Carlin, C.R. (2013). Epithelial to mesenchymal transition promotes breast cancer progression via a fibronectin-dependent STAT3 signaling pathway. J. Biol. Chem. *288*, 17954–17967.

Barretina, J., Caponigro, G., Stransky, N., Venkatesan, K., Margolin, A.A., Kim, S., Wilson, C.J., Lehár, J., Kryukov, G.V., Sonkin, D., et al. (2012). The Cancer Cell Line Encyclopedia enables predictive modelling of anticancer drug sensitivity. Nature *483*, 603–607.

Davis, S., Vanhoutte, P., Pagès, C., Caboche, J., and Laroche, S. (2000). The MAPK/ERK cascade targets both Elk-1 and cAMP response element-binding protein to control long-term potentiation-dependent gene expression in the dentate gyrus in vivo. J. Neurosci. *20*, 4563–4572.

Deka, J., Wiedemann, N., Anderle, P., Murphy-Seiler, F., Bultinck, J., Eyckerman, S., Stehle, J.-C., André, S., Vilain, N., Zilian, O., et al. (2010). Bcl9/Bcl9l are critical for Wnt-mediated regulation of stem cell traits in colon epithelium and adenocarcinomas. Cancer Res. *70*, 6619–6628.

Dissanayake, S.K., Wade, M., Johnson, C.E., O'Connell, M.P., Leotlela, P.D., French, A.D., Shah, K.V., Hewitt, K.J., Rosenthal, D.T., Indig, F.E., et al. (2007). The Wnt5A/protein kinase C pathway mediates motility in melanoma cells via the inhibition of metastasis suppressors and initiation of an epithelial to mesenchymal transition. J. Biol. Chem. *282*, 17259–17271.

Duncia, J.V., Santella, J.B., 3rd, Higley, C.A., Pitts, W.J., Wityak, J., Frietze, W.E., Rankin, F.W., Sun, J.H., Earl, R.A., Tabaka, A.C., et al. (1998). MEK inhibitors: the chemistry and biological activity of U0126, its analogs, and cyclization products. Bioorg. Med. Chem. Lett. *8*, 2839–2844.

Freissmuth, M., Boehm, S., Beindl, W., Nickel, P., Ijzerman, A.P., Hohenegger, M., and Nanoff, C. (1996). Suramin analogues as subtype-selective G protein inhibitors. Mol. Pharmacol. *49*, 602–611.

Fuchs, B.C., Fujii, T., Dorfman, J.D., Goodwin, J.M., Zhu, A.X., Lanuti, M., and Tanabe, K.K. (2008). Epithelial-to-mesenchymal transition and integrin-linked kinase mediate sensitivity to epidermal growth factor receptor inhibition in human hepatoma cells. Cancer Res. *68*, 2391–2399.

Giles, R.H., van Es, J.H., and Clevers, H. (2003). Caught up in a Wnt storm: Wnt signaling in cancer. Biochim. Biophys. Acta *1653*, 1–24.

Grumolato, L., Liu, G., Mong, P., Mudbhary, R., Biswas, R., Arroyave, R., Vijayakumar, S., Economides, A.N., and Aaronson, S.A. (2010). Canonical and noncanonical Wnts use a common mechanism to activate completely unrelated coreceptors. Genes Dev. *24*, 2517–2530.

Gujral, T.S., Peshkin, L., and Kirschner, M.W. (2014). Exploiting polypharmacology for drug target deconvolution. Proc. Natl. Acad. Sci. USA *111*, 5048–5053.

Guo, L., Chen, C., Shi, M., Wang, F., Chen, X., Diao, D., Hu, M., Yu, M., Qian, L., and Guo, N. (2013). Stat3-coordinated Lin-28-let-7-HMGA2 and miR-200-ZEB1 circuits initiate and maintain oncostatin M-driven epithelial-mesenchymal transition. Oncogene *32*, 5272–5282.

Gupta, P.B., Chaffer, C.L., and Weinberg, R.A. (2009). Cancer stem cells: mirage or reality? Nat. Med. *15*, 1010–1012.

Gupta, S., Iljin, K., Sara, H., Mpindi, J.P., Mirtti, T., Vainio, P., Rantala, J., Alanen, K., Nees, M., and Kallioniemi, O. (2010). FZD4 as a mediator of ERG oncogene-induced WNT signaling and epithelial-to-mesenchymal transition in human prostate cancer cells. Cancer Res. *70*, 6735–6745.

Harrison, C., Kiladjian, J.J., Al-Ali, H.K., Gisslinger, H., Waltzman, R., Stalbovskaya, V., McQuitty, M., Hunter, D.S., Levy, R., Knoops, L., et al. (2012). JAK inhibition with ruxolitinib versus best available therapy for myelofibrosis. N. Engl. J. Med. *366*, 787–798.

He, L., Isselbacher, K.J., Wands, J.R., Goodman, H.M., Shih, C., and Quaroni, A. (1984). Establishment and characterization of a new human hepatocellular carcinoma cell line. In Vitro *20*, 493–504.

Jordan, N.V., Prat, A., Abell, A.N., Zawistowski, J.S., Sciaky, N., Karginova, O.A., Zhou, B., Golitz, B.T., Perou, C.M., and Johnson, G.L. (2013). SWI/SNF chromatin-remodeling factor Smarcd3/Baf60c controls epithelial-mesenchymal transition by inducing Wnt5a signaling. Mol. Cell. Biol. *33*, 3011–3025.

Katada, T. (2012). The inhibitory G protein G(i) identified as pertussis toxin-catalyzed ADP-ribosylation. Biol. Pharm. Bull. *35*, 2103–2111.

Klaus, A., and Birchmeier, W. (2008). Wnt signalling and its impact on development and cancer. Nat. Rev. Cancer *8*, 387–398.

Lee, J.M., Dedhar, S., Kalluri, R., and Thompson, E.W. (2006). The epithelial-mesenchymal transition: new insights in signaling, development, and disease. J. Cell Biol. *172*, 973–981.

Lenaerts, T., Ferkinghoff-Borg, J., Stricher, F., Serrano, L., Schymkowitz, J.W.H., and Rousseau, F. (2008). Quantifying information transfer by protein domains: analysis of the Fyn SH2 domain structure. BMC Struct. Biol. *8*, 43.

Li, C., Chen, H., Hu, L., Xing, Y., Sasaki, T., Villosis, M.F., Li, J., Nishita, M., Minami, Y., and Minoo, P. (2008). Ror2 modulates the canonical Wnt signaling in lung epithelial cells through cooperation with Fzd2. BMC Mol. Biol. *9*, 11.

Lin, S., Baye, L.M., Westfall, T.A., and Slusarski, D.C. (2010). Wnt5b-Ryk pathway provides directional signals to regulate gastrulation movement. J. Cell Biol. *190*, 263–278.

Luttrell, D.K., and Luttrell, L.M. (2004). Not so strange bedfellows: G-protein-coupled receptors and Src family kinases. Oncogene *23*, 7969–7978.

Mariotti, A., Kedeshian, P.A., Dans, M., Curatola, A.M., Gagnoux-Palacios, L., and Giancotti, F.G. (2001). EGF-R signaling through Fyn kinase disrupts the function of integrin alpha6beta4 at hemidesmosomes: role in epithelial cell migration and carcinoma invasion. J. Cell Biol. *155*, 447–458.

O'Shea, J.J., Gadina, M., and Schreiber, R.D. (2002). Cytokine signaling in 2002: new surprises in the Jak/Stat pathway. Cell Suppl. *109*, S121–S131.

Paul, S., and Roblin, X. (2012). Tofacitinib in active ulcerative colitis. N. Engl. J. Med. *367*, 1959–1960, author reply 1960–1961.

Payne, G., Shoelson, S.E., Gish, G.D., Pawson, T., and Walsh, C.T. (1993). Kinetics of p56lck and p60src Src homology 2 domain binding to tyrosine-phosphorylated peptides determined by a competition assay or surface plasmon resonance. Proc. Natl. Acad. Sci. USA *90*, 4902–4906.

Savagner, P. (2010). The epithelial-mesenchymal transition (EMT) phenomenon. Ann. Oncol. *21* (*Suppl 7*), vii89–vii92.

Scheel, C., Eaton, E.N., Li, S.H.-J., Chaffer, C.L., Reinhardt, F., Kah, K.-J., Bell, G., Guo, W., Rubin, J., Richardson, A.L., and Weinberg, R.A. (2011). Paracrine and autocrine signals induce and maintain mesenchymal and stem cell states in the breast. Cell *145*, 926–940.

Schust, J., Sperl, B., Hollis, A., Mayer, T.U., and Berg, T. (2006). Stattic: a small-molecule inhibitor of STAT3 activation and dimerization. Chem. Biol. *13*, 1235–1242.

Sleeman, J., and Steeg, P.S. (2010). Cancer metastasis as a therapeutic target. Eur. J. Cancer *46*, 1177–1180.

Takahashi, K., and Yamanaka, S. (2006). Induction of pluripotent stem cells from mouse embryonic and adult fibroblast cultures by defined factors. Cell *126*, 663–676.

Tarcic, G., Avraham, R., Pines, G., Amit, I., Shay, T., Lu, Y., Zwang, Y., Katz, M., Ben-Chetrit, N., Jacob-Hirsch, J., et al. (2012). EGR1 and the ERK-ERF axis drive mammary cell migration in response to EGF. FASEB J. *26*, 1582–1592.

Teng, T.S., Lin, B., Manser, E., Ng, D.C.H., and Cao, X. (2009). Stat3 promotes directional cell migration by regulating Rac1 activity via its activator betaPIX. J. Cell Sci. *122*, 4150.

Thiery, J.P., Acloque, H., Huang, R.Y., and Nieto, M.A. (2009). Epithelial-mesenchymal transitions in development and disease. Cell *139*, 871–890.

Weigelt, B., Peterse, J.L., and van 't Veer, L.J. (2005). Breast cancer metastasis: markers and models. Nat. Rev. Cancer *5*, 591–602.

Wen, Z., and Darnell, J.E., Jr. (1997). Mapping of Stat3 serine phosphorylation to a single residue (727) and evidence that serine phosphorylation has no influence on DNA binding of Stat1 and Stat3. Nucleic Acids Res. *25*, 2062–2067.

Wen, Z., Zhong, Z., and Darnell, J.E., Jr. (1995). Maximal activation of transcription by Stat1 and Stat3 requires both tyrosine and serine phosphorylation. Cell *82*, 241–250.

Willert, K., Brown, J.D., Danenberg, E., Duncan, A.W., Weissman, I.L., Reya, T., Yates, J.R., 3rd, and Nusse, R. (2003). Wnt proteins are lipid-modified and can act as stem cell growth factors. Nature *423*, 448–452.

Wilson, T.R., Fridlyand, J., Yan, Y., Penuel, E., Burton, L., Chan, E., Peng, J., Lin, E., Wang, Y., Sosman, J., et al. (2012). Widespread potential for growth-factor-driven resistance to anticancer kinase inhibitors. Nature *487*, 505–509.

Wu, Z.-Q., Brabletz, T., Fearon, E., Willis, A.L., Hu, C.Y., Li, X.-Y., and Weiss, S.J. (2012). Canonical Wnt suppressor, Axin2, promotes colon carcinoma oncogenic activity. Proc. Natl. Acad. Sci. USA *109*, 11312–11317.

Ye, Q.H., Qin, L.X., Forgues, M., He, P., Kim, J.W., Peng, A.C., Simon, R., Li, Y., Robles, A.I., Chen, Y., et al. (2003). Predicting hepatitis B virus-positive metastatic hepatocellular carcinomas using gene expression profiling and supervised machine learning. Nat. Med. *9*, 416–423.